The interaction between a plane shear layer and a slender body

Parviz Merati
Aircraft and Automotive Engineering, Western Michigan University, Kalamazoo, MI, USA

Ronald J. Adrian
Theoretical and Applied Mechanics, and Mechanical and Industrial Engineering, University of Illinois at Urbana Champaign, Urbana, IL, USA

The interaction of a plane shear layer with a thin flat plate located in the nonlinear region of the shear layer has been investigated experimentally. The shear layer's velocity ratio is 0.375, and its Reynolds number is $\rho\Delta U\theta_0/\mu=625$. It is found that for different angles of attack of the plate, the mixing layer is deflected toward the slower stream. In addition, the plate attenuates turbulent fluctuations of the shear layer structures.

Keywords: turbulent shear layer; impingement; slender body; disturbing plate

Introduction

Free shear flows are often modified by the presence of surrounding objects. Oscillations of impinging free shear layers are the source of flow noise and undesirable structural loading. Some of the basic engineering applications are the impingement of shear layer flows with edge geometries such as mixing layer-edge, rectangular cavity, jet-plate, and jet-edge.

In recent years, there have been numerous efforts to simulate or model impinging shear layers. Rogler[1] attempted to understand the effect of incident free stream turbulence on semi-infinite flat plates by modeling the interaction of a flat plate with an array of square-type spanwise vortices distributed uniformly throughout space. He concluded that the bisection of a vortex as it encounters the plate yields a pair of vortices that rotate in the same direction. The combined height of these vortices is less than the height of the original vortex. Small segments of a vortex that has been cut by the plate, but not through its center, are completely absorbed by neighboring vortices.

Conlisk and Rockwell[2] modeled the vortex-corner interaction using point vortices. They concentrated on the interaction of an irregularly spaced pattern of discrete vortices with a flat plate, a bluff body, and a forward-facing step. Modeling studies by Conlisk and Rockwell[2] showed that the dimensionless amplitude of the pressure fluctuation at the impinging surface is highly sensitive to variations of the initial position of the incoming vortices, and to a large extent insensitive to variations of its strength. Most importantly, Conlisk and Rockwell[2] could determine the form of the time-average pressure and velocity spectra if the patterns of vortices upstream of the corner were prescribed. However, the main shortcomings of their method are associated with distributed vorticity inherent in laboratory vortices and the severing of vortices at the impingement surface. The impingement of shear layer flows is reviewed by Rockwell.[3]

Address reprint requests to Dr. Merati at Western Michigan University, Kalamazoo, MI 49008-5065, USA.

Received 30 September 1990; accepted 10 April 1991

Knisely and Rockwell,[4] in their study of the impinging shear layer on a cavity corner, observed that successive vortices arose from the amplified instability wave, underwent organized variations in impingement location (y-direction), and produced low frequency components of corner pressure. The spectral content and instantaneous traces of the impingement pressure were consistent with those fluctuations near the shear layer separation edge, which is evidence of strong upstream influence of the corner region. They concluded that for larger impingement lengths, the upstream influence from the impingement edge is considerably weaker.

Merati and Adrian[5] predicted the upstream effect of the impingement of free shear layers on a solid boundary located in the region of linear instabilities. They found that disturbances from the vicinity of the disturbing plate's leading edge feed back into the initial disturbance field of the shear layer to significantly alter its amplitude, increasing it at certain frequencies and suppressing it by negative feedback at other frequencies.

Savill and Mumford[6] have investigated the interaction between flat plate turbulence manipulators and the hairpin eddy structure of the boundary layer. It has been shown that the skin friction reduction behind such devices is due to several active mechanisms as well as the passive effect of the imposed momentum deficit. It appeared that an interaction between the introduced wake vortices, of opposite sign to the mean vorticity, and the near wall flow played the dominant role.

Most of the previous studies on impinging shear layers were concentrated on the interaction of a shear layer with the leading edge of a downstream body. The purpose of the present study is to investigate the behavior of a shear layer in the entire neighborhood of a thin flat plate with different angles of attack. This study is performed in the impingement region, plate region, and wake region of the plate. In addition, the effect on the shear layer of the plate offset and its length are investigated. Behavior of the nonimpinging shear layer has been studied experimentally for the purpose of comparison with the impinging shear layer. An understanding of the entire flow field is needed to evaluate the flow disturbances that are fed back from the flow-plate interaction to the highly receptive initial region of the shear layer.

Experimental facility and procedures

Experiments were performed in a two-stream plane shear layer wind tunnel (Figure 1). The two streams were formed by dividing a single stream with a splitter plate and reducing the speed of the lower stream with fabric that created appropriate pressure drop. The velocities of the upper and lower streams were

$U_1 = 7.31\ \text{ms}^{-1}$ and $U_2 = 2.74\ \text{ms}^{-1}$

respectively, yielding a velocity ratio $U_2/U_1 = 0.375$.

The boundary layer momentum thickness of the faster and slower streams measured 2 mm downstream of the splitter plate separation edge were $\theta_{01} = 1.1$ mm and $\theta_{02} = 0.95$ mm, respectively. Reynolds numbers based on $\Delta U = U_1 - U_2$ and $\theta_0 = \theta_{01} + \theta_{02}$ were $\rho \Delta U \theta_0/\mu = 625$ and $\rho U_1 \theta_0/\mu = 999$. The splitter plate reduced from 3.2-mm thickness to a knife-sharp separation edge over a distance of 76 mm. The shear layer was enclosed in a 830-mm Plexiglas test section with a 380×510 mm cross section.

The boundary layers on the splitter plate were not tripped to generate turbulent boundary layers. Laminar flow behavior in the initial region of the shear layer observed from the flow photographs of Figure 2 show that the boundary layers on the

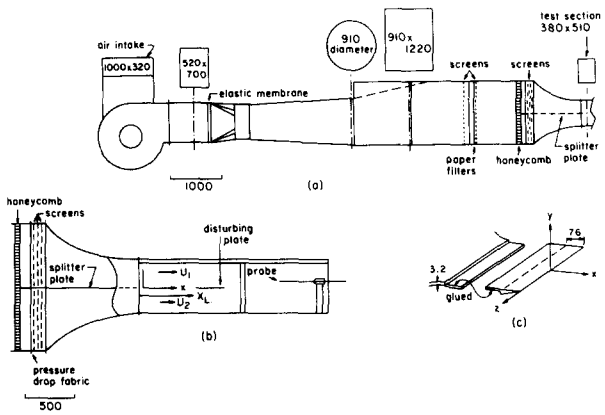

Figure 1 (a) Schematic of the wind tunnel. (b) The contraction cone and the test section. (c) The knife edge (all dimensions in millimeters)

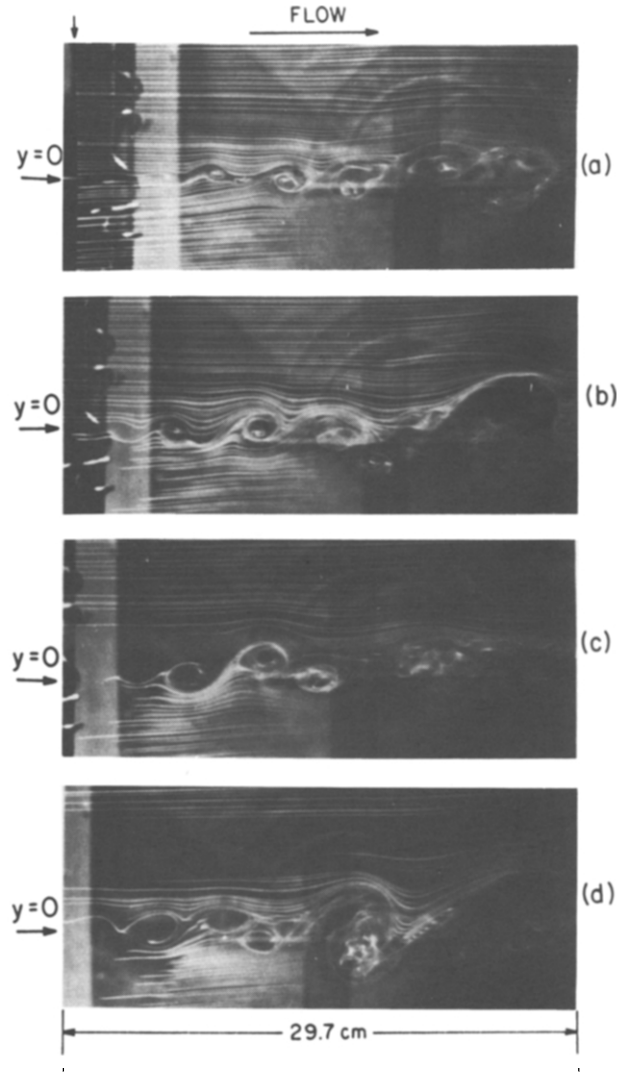

Figure 2 Photographs of the visualized flow of the shear layer

Notation

A, B, C, D, E, F	Different disturbing plates
t_p	Disturbing plate thickness
U	Streamwise velocity
V	Vertical velocity
U_1	Streamwise velocity in the faster stream
U_2	Streamwise velocity in the slower stream
x	Streamwise direction
x_L	x-coordinate of the disturbing plate leading edge
x_p	x-coordinate of the disturbing plate midspan
y	Vertical direction, perpendicular to x axis
y_L	y-coordinate of the disturbing plate leading edge
y_p	y-coordinate of the disturbing plate midspan
z	An axis perpendicular to x and y axes
z_L	z-coordinate of the disturbing plate leading edge
z_p	z-coordinate of the disturbing plate midspan
Greek symbols	
ΔU	$U_2 - U_1$
θ_{01}	Momentum thickness measured 2 mm downstream of the splitter plate in the faster stream
θ_{02}	Momentum thickness measured 2 mm downstream of the splitter plate in the slower stream
θ_0	$\theta_{01} + \theta_{02}$
μ	Dynamic viscosity of air
ρ	Mass density of air
σ_u	Root mean square value of the streamwise velocity fluctuations
σ_v	Root mean square value of the vertical velocity fluctuations
ϕ	Angle of attack of the disturbing plate

splitter plate were laminar. Flow photographs obtained at different stations in the cross-streamwise direction showed a two-dimensional shear layer.

Spectrum measurement of the streamwise velocity near the initial region of the shear layer showed that the most amplified disturbance was 180 Hz.

Streamwise and cross-streamwise velocity measurements were obtained by a TSI Model 1241-T1.5 × hot-wire probe. The distance between the two sensors was 1 mm. Each sensor was 4 μ in diameter and had a 1.25-mm active length. The probe was mounted on a long, 4.6-mm diameter horizontal probe support, which was supported at its downstream end by a rigid, 3.2-mm thick vertical steel arm designed to minimize flow disturbances. A 6.35-mm diameter movable brace extending across the test section well below the shear layer stiffened the vertical arm and eliminated vibrations.

Two TSI 1050 anemometers with a 5:1 bridge ratio and a 100 kHz low pass output filter were used. The overheat ratio and the optimum frequency response for each sensor were set at 1.7 and 7.5 μsec, respectively. For each sensor, a TSI 1057 signal conditioner was used to subtract DC voltage for obtaining better dynamic range for the fluctuating part of the signal. After subtracting the DC voltage, the signal was amplified 10 times before digitization. Typical minimum and maximum rms voltages before digitization were 0.28 and 6 v, respectively. Mean voltages were obtained by averaging the total signal without filtering and were added to the filtered readings to recover the full signal. At each location, 10,240 data at 4,000 Hz sampling rate were acquired. The data were stored on floppy diskettes for later analysis using a special program developed to obtain mean and turbulence intensities in the two directions.

Flow visualization was performed using the smoke-wire technique with a vertical 0.0762-mm diameter wire.

The flow was studied around six disturbing plates A, B, C, D, E, and F, with streamwise length of 127, 100, 80, 60, 40, and 20 mm, respectively. Each plate was positioned downstream of the splitter plate separation edge and extended across the width of the test section. The thickness of each plate was 2 mm, and the shape of each leading edge was a linear taper from 0.2 to 2 mm over a distance of 20 mm.

Development of the nonimpinging shear layer

Photographs of the shear layer are shown in Figure 2. The separation edge of the splitter plate located at the left side of the flow photographs of Figure 2 is marked with an arrow. Flow photographs were taken at widely separated times. Instability waves, their roll-up into vortices, and their growth are shown clearly. The well-known vortex pairing phenomena is evident in Figure 2c where an upstream vortex catches a downstream vortex. The new vortex formed by merging of the smaller vortices has a passage frequency of one-half of the original frequency. The lower frequency resulting from coalescence in the region of flow well upstream of merging has been detected previously by Ho and Nosseir.[7]

Streamwise mean velocity profiles of the shear layer from $x=0.2$ cm to $x=23$ cm are shown in Figure 3. The mean velocity profiles change with downstream distance immediately after the trailing edge of the splitter plate. At $x=0.2$ cm, the two boundary layers merge into a wake flow, which persists up to $x=4.0$ cm.

Streamwise turbulence intensity profiles from $x=0.2$ cm to $x=23.0$ cm are shown in Figure 4. The location of the maximum turbulence intensity moves toward $y=0$ as the flow develops downstream. The growth of the shear layer is indicated by existence of thicker turbulence intensity profiles as the flow develops downstream.

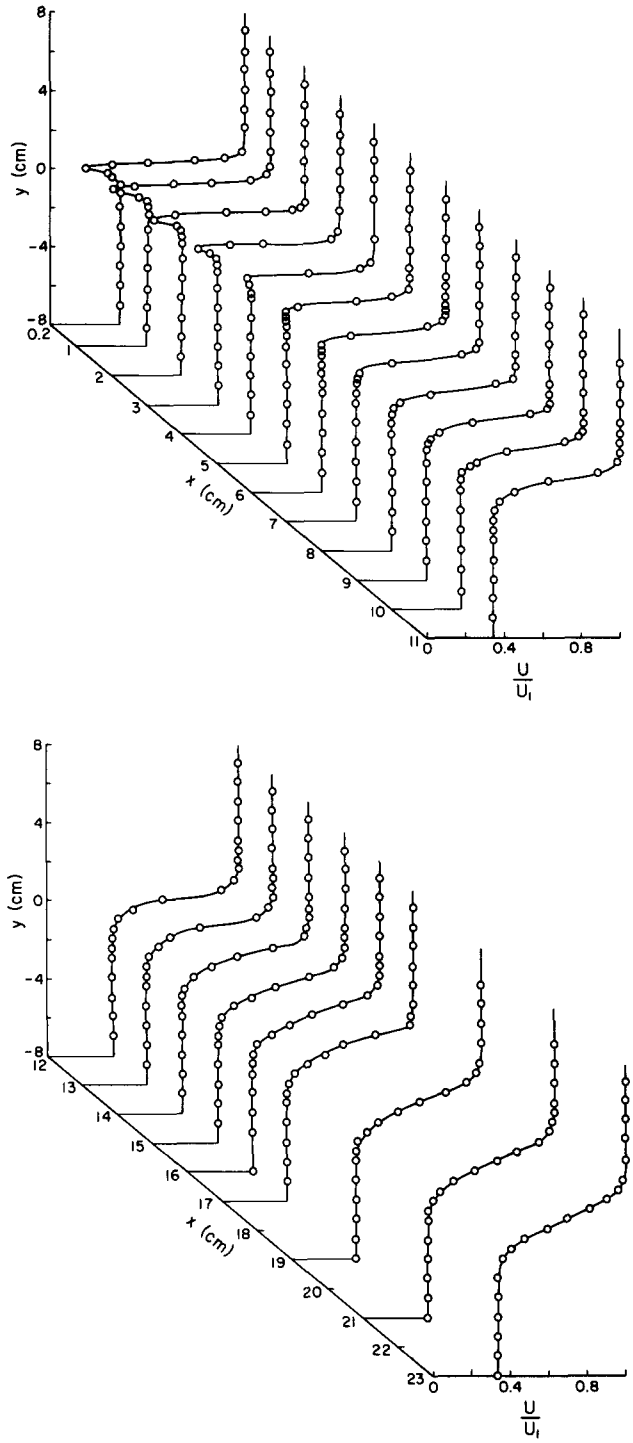

Figure 3 Streamwise mean velocity profiles at different locations in the test section of the plane shear layer tunnel

The spread of the mixing layer is represented by the variation in the shear layer momentum thickness θ defined by the following relationship

$$\theta=\int_{-\infty}^{+\infty}\frac{U}{U_1}\left(1-\frac{U}{U_1}\right)dy$$

where U is the mean velocity at each y location. In practice, the integration is extended over the thickness of the shear layer. The momentum thickness at $x=0$ is obtained for the faster

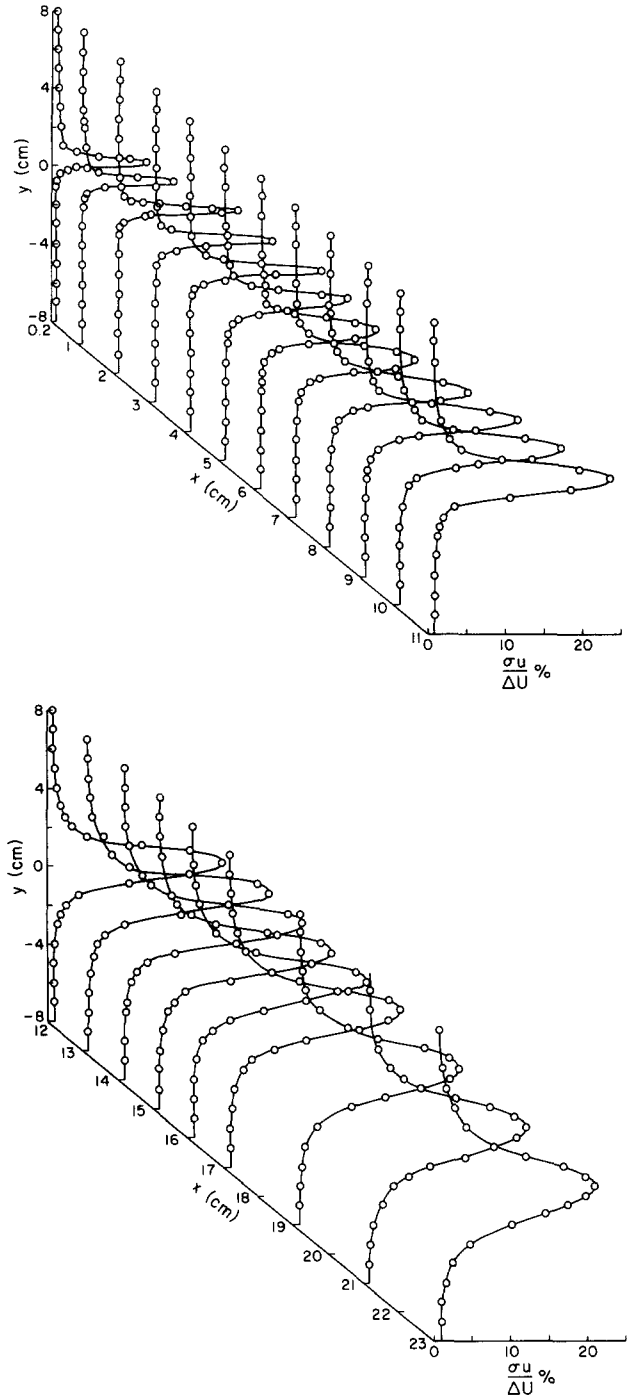

Figure 4 Streamwise turbulence intensity profiles at different locations in the test section of the plane shear layer tunnel

stream and is defined by

$$\theta_{01} = \int_0^\infty \frac{U}{U_1}\left(1-\frac{U}{U_1}\right) dy$$

The shear momentum thickness θ as the flow develops downstream is shown in Figure 5. The more rapid growth of the shear layer thickness downstream of $x=4$ cm compared with its growth in the linear region ($0<x<4$ cm) indicates the presence of the merging process in the nonlinear region. The merging process is accompanied by the entrainment of the potential fluid into the mixing layer and thickening of the shear layer.

Previous studies performed in the same shear layer by Merati and Adrian[5] indicated a region for exponential growth of background disturbances up to 4 cm downstream of the separation edge of the splitter plate. This region was followed by nonlinear distortion involving energy transfer between the fundamental and its higher harmonics.

Impinging shear layer

This section describes interaction of the plane shear layer with a thin flat plate located in the nonlinear region of the shear layer. Flow fields in the shear layer with and without a flat plate are compared. As a result of this comparison, three distinct regions of flow field are observed: the region between the shear layer separation edge and the leading edge of the plate, called impingement region; the flow between the plate leading edge and its trailing edge, called the plate region; and flow downstream of the plate trailing edge, called wake region. Flow behavior in the impingement, plate, and wake regions is described in the next three sections.

The mixing layer and the downstream plate are shown schematically in Figure 6. The streamwise mean flow direction is represented by x-axis, and y-axis is in the vertical direction and is perpendicular to x-axis. The midspan of the mixing layer separation edge is represented by $x=y=z=0$. x_p, y_p, and z_p are the coordinates of the plate centroid and ϕ is the plate rotation angle around an axis passing through x_p, y_p, z_p and parallel to the z-axis.

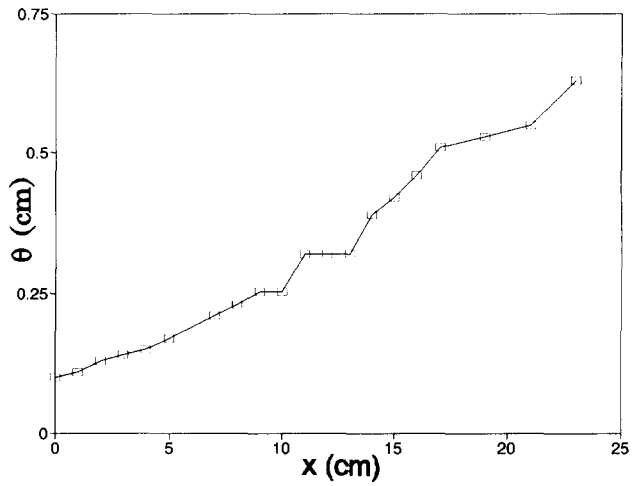

Figure 5 Momentum thickness for the shear layer

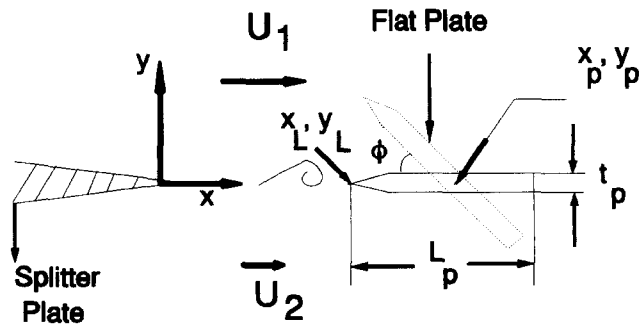

Figure 6 Schematic of the shear layer with a downstream plate

Impingement region

Photographs of the shear layer with the plate A inserted at different downstream locations and constant $y=0.0$ are shown in Figure 7. The plate thickness $t_p=2$ mm is indicated in Figure 7a. The plate appears thicker in the photographs since its front edge is out of focus. The camera is focused on the mid-span of the plate.

The flow photographs of Figure 7 show that vortices are cut by the plate leading edge. A secondary counter-rotating vortex is expected to be induced along the flat plate. However, this secondary flow is not observed clearly in the flow photographs of Figure 7. Vortex coalescence occurs in the impingement region as shown in Figure 7e and in other flow photographs not presented here.

Streamwise and vertical mean velocity profiles at $x=10$ cm and $x=13$ cm for plate A located in the $x-z$ plane ($x_L=13$ cm, $y_L=0$) are compared with the corresponding profiles for the nonimpinging shear layer in Figure 8.

Neither U nor V profiles at $x=10$ cm show any significant change due to presence of the plate. At the plate leading edge, the U profile in absence of the plate shows a narrower and steeper shear region. The plate divides the flow, directing more below the plate than above. The stagnation region around the leading edge of the plate as shown in Figure 8d causes larger upward mean flow, V, above the plate and larger downward mean flow below the plate compared with the no-plate condition. The effect of the plate extends over an approximate range of 6 cm, -4 cm $< y < 2$ cm, i.e., 30 times larger than the plate thickness.

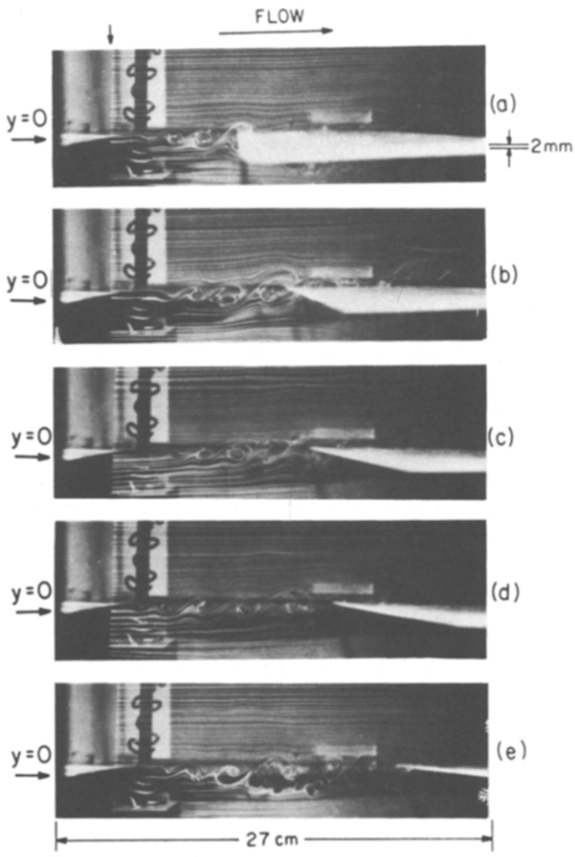

Figure 7 Photographs of the visualized flow of the shear layer and plate A, with its leading edge located at $y_L=0.0$: (a) $x_L=9$ cm, (b) $x_L=13$ cm, (c) $x_L=15$ cm, (d) $x_L=17$ cm, (e) $x_L=22.5$ cm

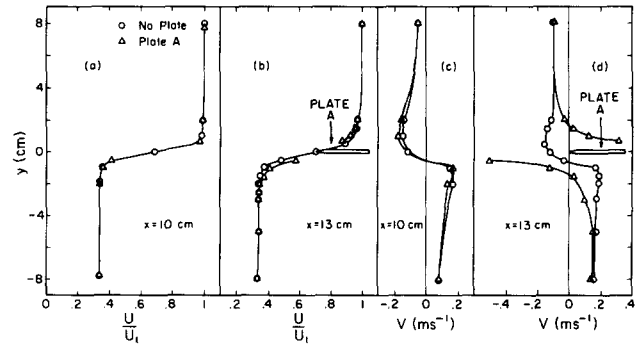

Figure 8 Streamwise and vertical mean velocity profiles (U, V) in the presence and absence of plate A ($x_L=13$ cm, $y_L=0.0$): (a) and (c) $x=10$ cm; (b) and (d) $x=13$ cm

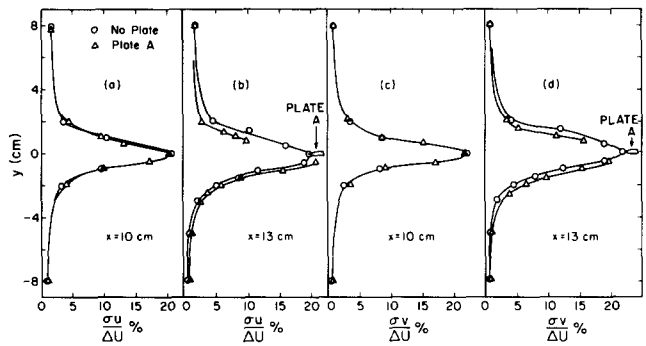

Figure 9 Streamwise and vertical turbulence intensity profile (σ_u, σ_v) in the presence and absence of plate A ($x_L=13$ cm, $y_L=0.0$): (a) and (c) $x=10$ cm; (b) and (d) $x=13$ cm

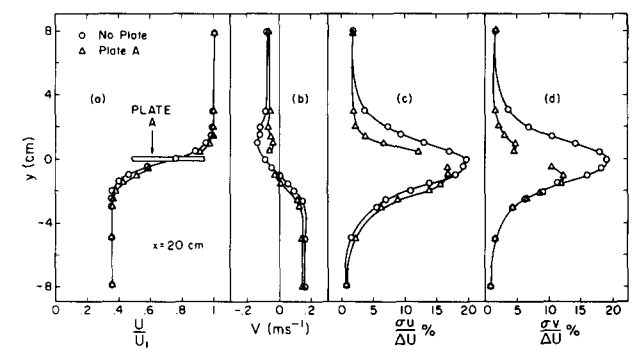

Figure 10 (a) Streamwise mean velocity, (b) vertical mean velocity, (c) streamwise turbulence intensity, (d) vertical turbulence intensity profiles in the plate region at $x=20$ cm; plate A ($x_L=13$ cm, $y_L=0.0$)

Streamwise and vertical velocity turbulence intensity profiles σ_u and σ_v at $x=10$ and 13 cm for plate A ($x_L=13$ cm, $y_L=0$) are compared with the corresponding profiles in the absence of the plate in Figure 9. The σ_u and σ_v profiles at $x=10$ cm do not show any change due to presence of the plate. At the plate leading edge, the streamwise and vertical turbulence intensity profiles are shifted toward the slower stream compared with the same profiles in absence of the plate.

Plate region

The streamwise mean velocity profile at $x=20$ cm with the plate A present is compared with the corresponding profile for the nonimpinging shear layer in Figure 10a. The width of the shear layer is not affected by the plate at $x=20$ cm. However, the plate causes the shear layer to shift downward approximately

4 mm at $x=20$ cm. Above the plate, the streamwise mean velocity profile is considerably more uniform at $x=20$ cm compared with the corresponding profile at $x=13$ cm. The entrained high speed potential flow from the faster stream causes an increase in the U component of the velocity in the flow region between $x=13$ cm and $x=20$ cm above the plate. The plate inhibits mixing of the two streams. Below the plate, the shear layer has grown similar to the no-plate condition except in the region $-2\text{ mm}<y<0$ where the flow has slowed down from the plate leading edge at $x=13$ cm to $x=20$ cm.

The vertical mean velocity profile V at $x=20$ cm with plate A present is compared with the corresponding profile for the nonimpinging shear layer as shown in Figure 10b. This comparison clearly shows that the presence of the plate inhibits mixing of the mean flow in the cross-streamwise direction.

Streamwise and vertical turbulence intensity profiles σ_u and σ_v at $x=20$ cm with plate A present are compared with the corresponding profiles for the nonimpinging shear layer in Figures 10c and 10d, respectively. The turbulence intensity profiles are shifted downward, and their values are decreased compared with the corresponding profiles for the nonimpinging shear layer. The decrease in turbulence intensities indicates large eddies are damped in presence of the plate. The larger decrease in the σ_v values compared with the σ_u values is due to vertical obstruction of the plate to flow motion.

Flow in the plate A region when $x_L=13$ cm, $y_L=0$, is shown by flow photographs of Figure 11. There is no plate in the visualized flow of Figure 11d. Vortices are divided by the plate and their different vertical locations with respect to the plate are shown in Figure 11. The organized structures are often directed toward the slower stream as observed by comparing flow photographs of Figures 11b and 11d. Flow is more turbulent below the plate compared with the flow above the plate, consistent with the turbulence intensity measurements at $x=20$ cm.

Trajectories of locations of the peak streamwise turbulence intensity and the peak vertical turbulence intensity with and without the plate are shown in Figures 12a and 12b, respectively. At $x=20$ cm, the plate causes a 9-mm downward movement of the peak vertical turbulence intensity that is larger than the 4-mm downward movement of the peak streamwise turbulence intensity. Thus, the cross-stream motion of the flow field is affected more by the plate than the streamwise motion.

Wake region

Streamwise and vertical velocity profiles at $x=28$ cm, i.e., 2.3 cm downstream of the plate trailing edge are compared with the corresponding profiles for the nonimpinging shear layer in Figures 13a and 13b, respectively. The shape of the streamwise mean velocity profile in the wake indicates existence of a new, thinner inner shear layer embedded in a larger outer shear layer. The larger values of V compared with the corresponding values

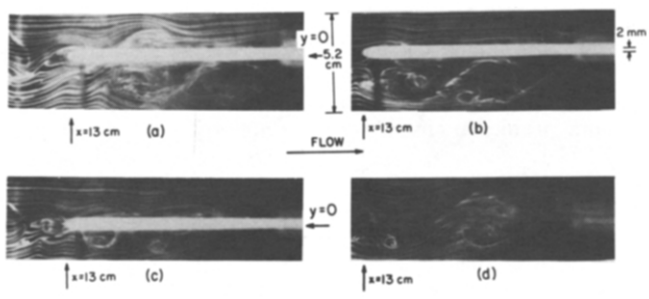

Figure 11 Photographs of the visualized flow of the shear layer (a), (b), and (c) plate A ($x_L=13$ cm, $y_L=0.0$), (d) no plate

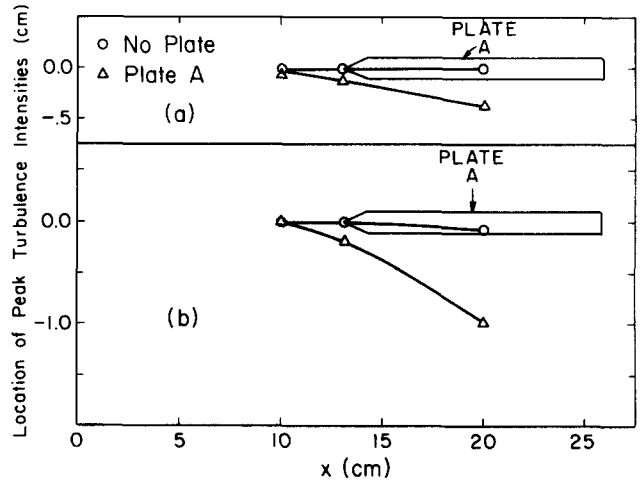

Figure 12 Trajectory of the peak (a) streamwise turbulence intensity, (b) vertical turbulence intensity; plate A ($x_L=13$ cm, $y_L=0.0$)

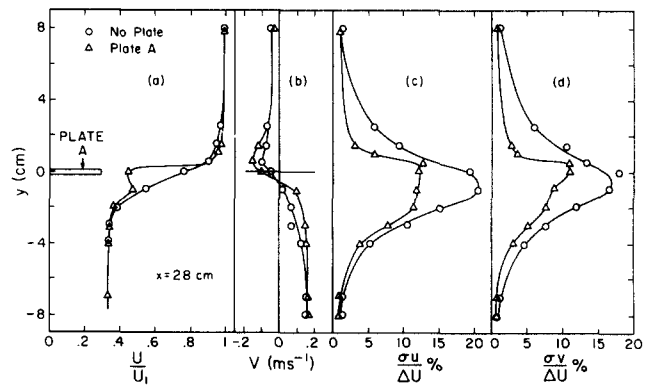

Figure 13 (a) Streamwise mean velocity, (b) vertical mean velocity, (c) streamwise turbulence intensity, (d) vertical turbulence intensity profiles in the wake of plate A ($x_L=13$ cm, $y_L=0.0$) at $x=28$ cm

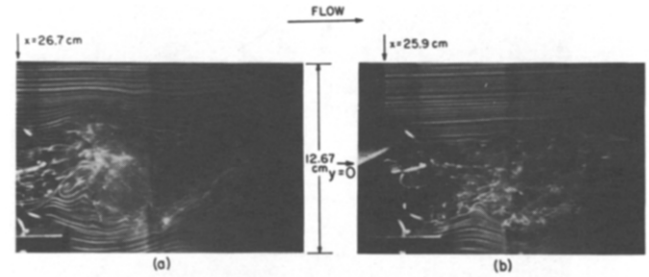

Figure 14 Photographs of flow of (a) nonimpinging shear layer, (b) wake of the plate; plate A ($x_L=13$ cm, $y_L=0.0$)

for the nonimpinging shear layer indicate more mixing downstream of the plate. This is in contrast with reduced mixing at $x=20$ cm when plate is present.

Streamwise and vertical turbulence intensity profiles at $x=28$ cm are compared with the corresponding profiles for the nonimpinging shear layer in Figures 13c and 13d, respectively. The turbulence intensities are decreased in the wake compared with the nonimpinging shear layer, implying the shear layer has been weakened by the plate. The larger values of turbulence intensities at $y\simeq 4$ mm are due to the steep shear in the streamwise mean velocity profile in the $0\leq y\leq 5$ mm region. This is consistent with presence of small-scale vortices on top of the mixing layer in the wake of the plate. These small vortices are observed in the flow photograph of Figure 14b.

Flow in the wake of plate A is compared with the non-impinging mixing layer in flow photographs of Figure 14. The plate trailing edge is shown in Figure 14b by an arrow, and its location $y=0$. The shear layer flow is less turbulent for $y>0$ compared with the nonimpinging shear flow. The small-scale organized structures are absent in the flow of the nonimpinging mixing layer.

Effect of offset, length and orientation of a flat plate

Photographs of the shear layer flow with plate A located horizontally with its leading edge at $x_L=9$ cm and $y_L=0.0$, $y_L=1.2$ cm, and $y_L=-1.2$ cm are shown in Figures 15b, 15c, and 15d, respectively. The nonimpinging mixing layer is shown in Figure 15a for comparison. The large spanwise vortical structures are deflected toward the slower stream when the leading edge of the plate is located at $y_L=1.2$ cm. The large structures are divided by the plate when $y_L=0$ and are deflected toward the faster stream when $y_L=-1.2$ cm. The driving force for the shear layer deflection is the pressure field of the stagnation region near the plate leading edge.

Photographs of the visualized flow of the shear layer with plates of different lengths (plates A, B, C, D, E, and F), each located horizontally with its leading edge at $x_L=13$ cm and

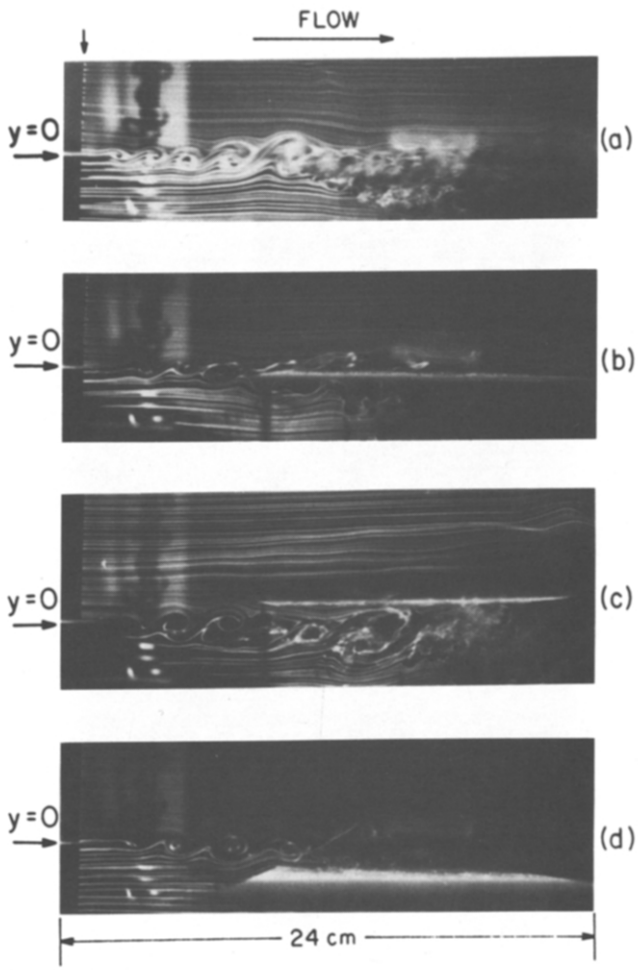

Figure 15 Photographs of the visualized flow of the shear layer with (a) no plate present, (b) plate A ($x_L=9$ cm, $y_L=0.0$), (c) plate A ($x_L=9$ cm, $y_L=1.2$ cm), (d) plate A ($x_L=9$ cm, $y_L=-1.2$ cm)

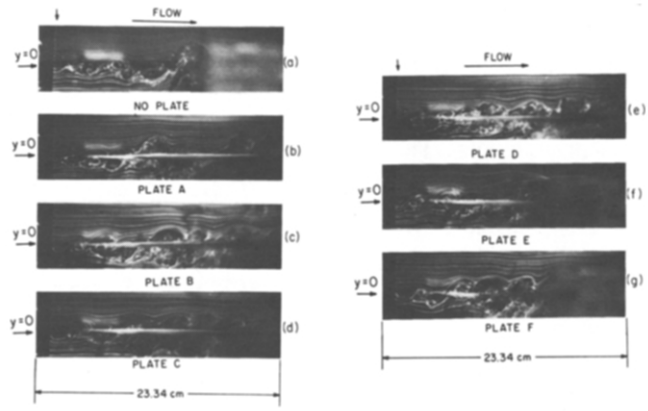

Figure 16 Photographs of the visualized flow of the shear layer with (a) no plate present, (b–g) plates of different length ($x_L=13$ cm, $y_L=0.0$)

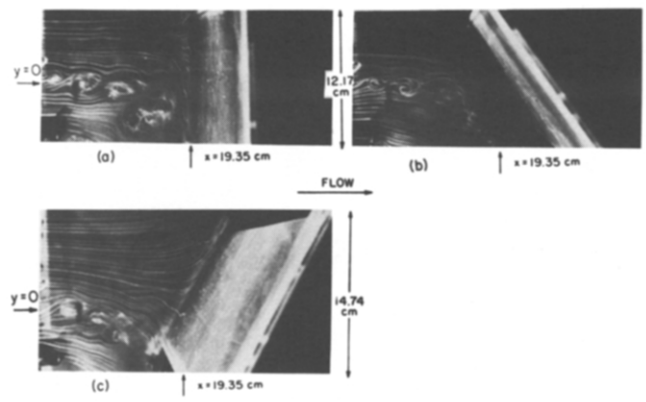

Figure 17 Photographs of the visualized flow of the shear layer with plate A ($x_p=19.4$ cm, $y_p=0.0$); (a) $\phi=90°$, (b) $\phi=60°$, (c) $\phi=120°$

$y_L=0$, are shown in Figure 16. These flow photographs do not reveal any significant difference in the impingement region due to the plate length. However, they do show that the plate disrupts normal development of the shear layer downstream of its leading edge. The large structures are often divided at different cross-streamwise positions, depending on the location of their impingement on the plate leading edge. They are also distorted due to possible presence of secondary vortices at the leading edge of the plate. At the trailing edge, two vortices, not necessarily parts of the same upstream vortex, sometimes merge, and flow develops downstream. The large structure resulting from this merger is disturbed further by flow in the wake of the plate.

Photographs of the mixing layer with plate A oriented at $\phi=90°$, 60°, and 120° are shown in Figures 17a, 17b, and 17c, respectively. The stagnation region is located in the faster stream and the vortices are deflected toward the slower stream for the three orientations. Deflection of the mixing layer toward the slower stream is controlled by potential flow in the faster stream, which results in a high pressure stagnation region. The stagnation region moves from the upper edge of the plate at $\phi=60°$ toward the lower edge as the plate rotates clockwise to 90° and subsequently to 120°. The photographs show that the potential flow from the faster stream inhibits impingement of the vortices on the plate. The vortices are severely distorted and at $\phi=90°$ are even pushed toward upstream.

Conclusions

A flat plate positioned in the nonlinear growth region of a plane shear layer interacts with the shear layer in several ways.

The plate leading edge generates large vertical velocities near its stagnation point. The effect of presence of the plate at zero angle of attack near its leading edge extends over a region that is 30 times larger than the plate thickness. Mixing of the mean flow is inhibited in a cross-streamwise direction near the middle of the plate.

The large structures are shifted toward the slower stream in the neighborhood of the plate. Turbulent fluctuations are damped by the plate.

At large angles of attack of the plate with respect to the incoming vortices, the mixing layer is deflected toward the slower stream by the high pressure field of the stagnation region generated by the impingement of the faster stream on the plate.

References

1 Rogler, H. The interaction between vortex-array representations of free-stream turbulence and semi-infinite flat plates. *J. Fluid Mech.*, 1978, **87**, 583–606

2 Conlisk, A. T., and Rockwell, D. Modeling of vortex-corner interaction using point vortices. *Phys. Fluids*, 1981, **24**, 2133–2142

3 Rockwell, D. Oscillations of impinging shear layers. *AIAA J.*, 1983, **21**, 645–664

4 Knisely, C., and Rockwell, D. Self-sustained low-frequency components in an impinging shear layer. *J. Fluid Mech.*, 1982, **116**, 157–186

5 Merati, P., and Adrian, R. J. Plane shear layer amplification by impingement on a slender body. AIAA 26th Aerospace Sciences Meeting, 1988, AIAA-88-0039

6 Savill, A. M., and Mumford, J. C. Manipulation of turbulent boundary layers by outer-layer devices: Skin-friction and flow-visualization results. *J. Fluid Mech.*, 1988, **191**, 389–418

7 Ho, C. M., and Nosseir, N. S. Dynamics of an impinging jet. I. The feedback phenomenon. *J. Fluid Mech.*, 1981, **105**, 119–142